A Matlab/Simulink Model of a Langevin's Ultrasonic Power Transducers

Igor Jovanović, Uglješa Jovanović and Dragan Mančić

***Abstract*— Ultrasonic sandwich transducer, also known as a Langevin's transducer, is a half-wave resonant structure that oscillates in thickness direction. In this paper, new Matlab/Simulink model of a prestressed unsymmetrical ultrasonic sandwich transducer is presented. The sandwich transducer is modeled by applying three-dimensional (3D) Matlab/Simulink models of piezoceramic rings and metal endings, which are derived based on the piezoceramic ring model recently proposed by the authors. By cascade connecting the piezoceramic rings model with metal endings model, a complete model of ultrasonic Langevin's transducer is obtained. Using this model one may determine any transducer transfer function, whereat is taken into the account the external medium influence, as well as the influence of the thickness and radial modes of each transducer component. The comparisons between experimental and theoretical results are quite good and validate the new design approach.**

***Index Terms*— Langevin's transducer, Matlab/Simulink model, 3D model, Resonance frequency characteristics.**

I. Introduction

Implementation of ultrasonic transducers began in 1917, when Paul Langevin designed the first piezoelectric sandwich transducer [1]. At the very beginning of its development, the basic application was in sonars. In nowadays, technological application of a power ultrasound is exploited in many branches of industry such as mining, ultrasonic machining, material processing, cutting, welding [2–4], sonochemistry [5,6] and other ultrasonic liquid processing applications [7].

Sandwich transducer, which is most often also called a Langevin's transducer, is a half-wave resonant structure that oscillates in thickness (longitudinal, extension, or axial) direction. In the simplest form, a sandwich transducer is consisted of an active layer or source of oscillations, made of one or more pairs of piezoceramic rings (Blocks 1 and 2, shown in Figure 1), mechanically compressed between metal endings by a bolt (Blocks 8, 9, 10 and 11, shown in Figure 1). For industry applications, the piezoceramic should possess a great electromechanical coupling factor, high Curie's temperature, low dielectric losses, and stable time and temperature properties. Metal endings are consisted of: a reflector (Blocks 5, 6 and 7, shown in Figure 1), which represents a rear part of the transducer, and an emitter (Blocks 3 and 4, shown in Figure 1), which transfers oscillations from source to an operating medium. Metal endings are most commonly made out of materials of different densities, in order to increase oscillation amplitudes on the operating surface of the emitter and decrease oscillation amplitudes on the reflector surface, as well as to improve the adjustment with the load.

Improvement of ultrasonic transducer performances requires a detailed investigation of the mechanical and electrical properties for different operating conditions. Modeling of more complete transducer constructions is not possible using one-dimensional model, which is based on solving the wave equation along the transducer. One-dimensional vibration theory is used where the longitudinal transducer dimension is greater than the lateral dimension, therefore only the thickness modes are considered and vibrations in other directions are neglected [8].

The research presented in this paper analyses the Matlab/Simulink 3D matrix model of the prestressed unsymmetrical ultrasonic sandwich transducer. Ultrasonic sandwich transducer is modelled using the approximate 3D matrix model previously proposed in paper [9], which takes into the account thickness and radial modes of oscillation as well as their mutual coupling. Piezoceramic rings are represented as networks with four mechanical and the single electrical contacts [10]. Similar approach is employed to model passive metal extensions based on the 3D matrix model of metal rings [11]. Metal parts are represented as networks with four or three contacts.

II. A Matlab/Simulink 3D Matrix Model of the Ultrasonic Transducer

This paper presents model of an ultrasonic sandwich transducer with a single pair of piezoceramic rings mechanically connected in series and electrically in parallel. By mutually connecting all transducer components in series and in parallel, a 3D electromechanical model of complete ultrasonic sandwich transducer is obtained (Figure 1). If an AC exiting voltage is applied on the electrical contacts while a proper ambient acoustic impedances are applied on the mechanical contacts it is possible to determine each transfer function of such system.

All model blocks are consisted of two basic parts. First one calculates all elements of the matrix model based on the inserted material properties. Second one solves system of equations using the calculated matrix model elements.

Models of piezoceramic rings consist of two blocks used to assign initial values of forces F_3 and F_4 acting from direction

Igor Jovanović, Uglješa Jovanović and Dragan Mančić are with the University of Niš, Faculty of Electronic Engineering, 14 Aleksandra Medvedeva, 18000 Niš, Serbia (e-mail: igor.jovanovic@elfak.ni.ac.rs, ugljesa.jovanovic@elfak.ni.ac.rs and dragan.mancic@elfak.ni.ac.rs).

of the second piezoceramic and reflector, which are obtained from Block 2 and Block 5 respectively. Based on the inserted ceramic properties, all elements are calculated $A_{i,j}=z_{i,j}(i,j=1,2,3,4,5)$ [9], along with all the necessary elements of system of equations (1):

$$\begin{bmatrix} 0 \\ 0 \\ E_3 \\ E_4 \\ E_5 \end{bmatrix} = \begin{bmatrix} A_{11} & A_{12} & A_{13} & A_{14} & A_{15} \\ 0 & a_{11} & a_{12} & a_{13} & a_{14} \\ 0 & 0 & b_{11} & b_{12} & b_{13} \\ 0 & 0 & 0 & c_{11} & c_{12} \\ 0 & 0 & 0 & c_{21} & c_{22} \end{bmatrix} \begin{bmatrix} v_1 \\ v_2 \\ v_3 \\ v_4 \\ I \end{bmatrix} \tag{1}$$

wherein:

$$\begin{aligned} a_{i,j} &= A_{1,j+1} \cdot A_{i+1,1} - A_{1,1} \cdot A_{i+1,j+1} \quad (i,j = 1,2,3,4) \\ b_{i,j} &= a_{1,j+1} \cdot a_{i+1,1} - a_{1,1} \cdot a_{i+1,j+1} \quad (i,j = 1,2,3) \\ c_{i,j} &= b_{1,j+1} \cdot b_{i+1,1} - b_{1,1} \cdot b_{i+1,j+1} \quad (i,j = 1,2) \end{aligned} \tag{2}$$

and:

$$\begin{aligned} E_3 &= A_{11}a_{11}F_1 \\ E_4 &= A_{11}a_{11}b_{12}F_3 - A_{11}a_{11}b_{11}F_4 \\ E_5 &= A_{11}a_{11}b_{31}F_3 - A_{11}a_{11}b_{11}U \end{aligned} \tag{3}$$

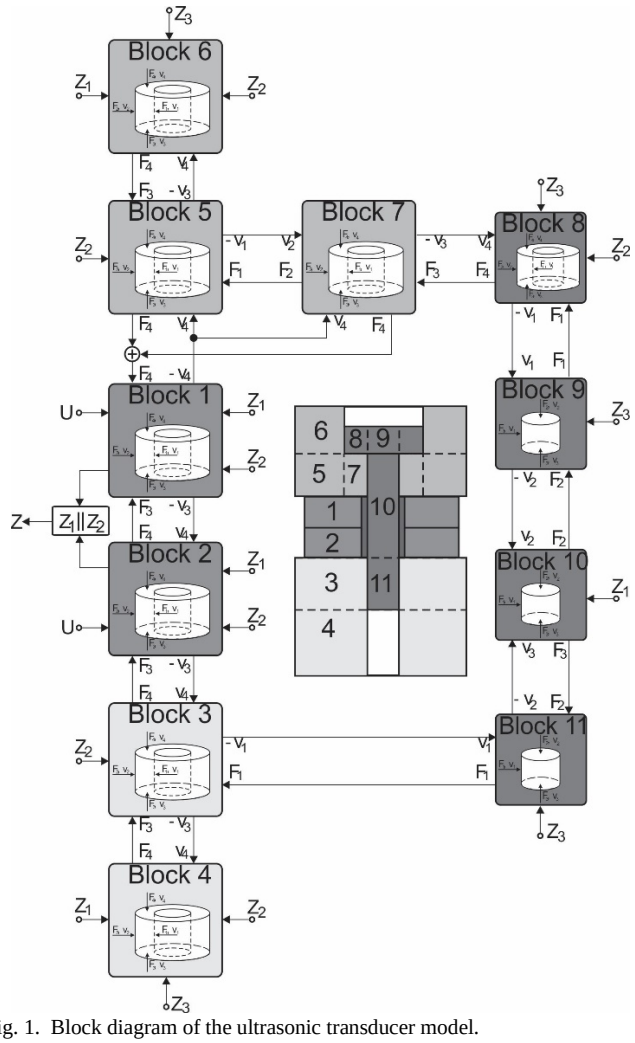

Fig. 1. Block diagram of the ultrasonic transducer model.

Difference between two models of piezoceramic rings, i.e. Block 1 and Block 2, is that the matrix of system of equations Block 2 (equation (4)) is different from the matrix of system of equations (1), hence the solution of the system of equations is different. This difference originates from the existence of contact ring-shaped surfaces between ceramics, i.e. knowing mechanical velocities on these surfaces, which are calculated in Block 1. Mechanical forces acting on the joint surfaces are the same while mechanical velocities have the same intensity but opposite directions.

$$\begin{bmatrix} 0 \\ 0 \\ E_3 \\ E_5 \end{bmatrix} = \begin{bmatrix} A_{11} & A_{12} & A_{13} & A_{14} & A_{15} \\ 0 & a_{11} & a_{12} & a_{13} & a_{14} \\ 0 & 0 & b_{11} & b_{12} & b_{13} \\ 0 & 0 & 0 & c_{21} & c_{22} \end{bmatrix} \begin{bmatrix} v_1 \\ v_2 \\ v_3 \\ v_4 \\ I \end{bmatrix} \tag{4}$$

Including the electrical impedance Z, which is from standpoint of the power supply connected in parallel to the electrical impedance of Block 1 (piezoelectric element), outputs of Block 2 are mechanical force and velocity acting on the ring-shaped surfaces towards the Block 1 ($F_4=A_{13}v_1+A_{23}v_2+A_{34}v_3+A_{44}v_4+A_{35}I$) and towards the transducer emitter ($-v_3$).

Models of the emitter and reflector are consisted of two parts described in Block 3 and Block 4 (emitter), and in Block 5 and Block 6 (reflector). Based on the geometrical properties of these components and their connection with the remaining transducer components, it can be concluded that models Block 4 and Block 6 are analogue. The same analogy applies to Block 3 and Block 5, with the only differences between them being their material properties and their geometrical dimensions. System of equations, which in the frequency domain characterizes Block 3, is given in expression (5), that is in expression (6) for Block 4:

$$\begin{bmatrix} F_1 \\ F_1A_{12} \\ H_3 \end{bmatrix} = \begin{bmatrix} A_{11} & A_{12} & A_{13} & A_{14} \\ 0 & a_{11} & a_{12} & a_{13} \\ 0 & 0 & b_{11} & b_{12} \end{bmatrix} \begin{bmatrix} v_1 \\ v_2 \\ v_3 \\ v_4 \end{bmatrix} \tag{5}$$

$$\begin{bmatrix} 0 \\ 0 \\ 0 \end{bmatrix} = \begin{bmatrix} A_{11} & A_{12} & A_{13} & A_{14} \\ 0 & a_{11} & a_{12} & a_{13} \\ 0 & 0 & b_{11} & b_{12} \end{bmatrix} \begin{bmatrix} v_1 \\ v_2 \\ v_3 \\ v_4 \end{bmatrix} \tag{6}$$

wherein $H_3=A_{11}a_{11}F_3+(A_{21}a_{21}-A_{31}a_{11})F_1$.

Mechanical velocities (v_1, v_2 and v_3) with the known velocity on the ring-shaped surface towards the piezoceramic (v_4), obtained from Block 2, are used to calculate the mechanical force F_4 acting towards the piezoceramic.

The obtained mechanical velocity on the ring-shaped surface towards the second part of the emitter v_3 is forwarded

to Block 4, wherein based on it and the acoustic input impedances F_4 force acting on that surface is calculated.

The central bolt is represented by Blocks 8, 9, 10 and 11. Due to the physical connections that appropriate central bolt parts have with the remaining transducer components, an analogy between Block 9 and Block 11 can be observed. Therefore, in the following text only Block 9 will be presented, whose outputs are mechanical velocities acting on the cylindrical surfaces towards the middle part of the central bolt, i.e. towards Block 10, and mechanical forces acting on the cylindrical surfaces of the central bolt towards the appropriate parts of the reflector that is the emitter. System of equations, which in the frequency domain characterizes Block 9 is given in expression (7).

$$\begin{bmatrix} F_2 \\ 0 \end{bmatrix} = \begin{bmatrix} A_{21} & A_{22} & A_{23} \\ A_{31} & A_{32} & A_{33} \end{bmatrix} \begin{bmatrix} v_1 \\ v_2 \\ v_3 \end{bmatrix} \tag{7}$$

Model of the middle part of the central bolt has the simplest structure. Using it in each simulation step the following instructions are performed: initialization of mechanical forces acting on the joint surfaces of all transducer components; calculation of mechanical velocities on the same surfaces using known values of ambient acoustic impedances acting on the appropriate transducer components; obtaining final and accurate initial mechanical forces. All aforementioned is performed using the circuit for solving equations (8).

$$\begin{aligned} v_1 &= \frac{A_{12}v_2 + A_{13}v_3}{-A_{11}} \\ F_2 &= A_{21}v_1 + A_{22}v_2 + A_{23}v_3 \\ F_3 &= A_{31}v_1 + A_{32}v_2 + A_{33}v_3 \end{aligned} \tag{8}$$

Mechanical connection of the ring-shaped reflector parts (Block 5 and Block 7), with the piezoelectric element (Block 1) is serial as can be seen in Figure 1. Their mutual connection in the transducer model is represented by the adder circuit of the reflector mechanical forces in the direction of the piezoelectric element, while value of mechanical velocity on the ring-shaped surface of the piezoelectric element is directly forwarded to the mentioned parts of the reflector.

Block 7 of the transducer model is used to solve system of equations (9) in which are known mechanical velocities v_2 and v_4 along with mechanical force F_3.

$$\begin{bmatrix} 0 \\ F_3 \end{bmatrix} = \begin{bmatrix} A_{11} & A_{12} & A_{13} & A_{14} \\ A_{31} & A_{32} & A_{33} & A_{34} \end{bmatrix} \begin{bmatrix} v_1 \\ v_2 \\ v_3 \\ v_4 \end{bmatrix} \tag{9}$$

After obtaining values of v_2 and v_4, the remaining mechanical forces are calculated as $F_2=A_{21}v_1+A_{22}v_2+A_{23}v_3+A_{24}v_4$ and $F_4=A_{41}v_1+A_{42}v_2+A_{43}v_3+A_{44}v_4$.

Ring-shaped part of the bolt head located above the reflector is in the model, opposed to the rest of the bolt, represented by the four-port network (Block 8) because of its physical dimensions (ring structure). In this block system of equations (5) is calculated, but in this case it applies $H_3=A_{21}a_{21}F_1\text{-}A_{31}a_{11}F_1$.

III. Results and Discussion

The calculated and experimental results are obtained using a PZT8 piezoceramic equivalent material [12] with dimensions Ø38/Ø15/5mm. The reflector and central bolt made out of stainless steel, its standard material parameters are density 7800kg/m^3, Poisson's ratio 0.29 and Young's modulus of elasticity $2.09\cdot10^{11}$N/m^2. The emitter is made out of duralumin, its standard material parameters are density 2790kg/m^3, Poisson's ratio 0.34 and Young's modulus of elasticity $0.68\cdot10^{11}$N/m^2. The electrical impedance measurements are done using HP4194A Impedance/Gain-Phase Analyzer.

In the following, the model is used to determine an input electrical impedance of the ultrasonic transducer, as well as mechanical impedances on the particular transducer outer surfaces. All blocks are masked (*mask-block*) and their properties are inserted in the window that appears by double clicking the corresponding block. Part of this window, in case of piezoceramic rings, is shown in Figure 2a, while the entire window in case of metal extensions is shown in Figure 2b. Figure 2a already shows inserted ceramic properties used in the laboratory. To insert properties of a non-predefined ceramic it necessary to select the "User-defined" option in the popup menu, this enables insertion of all ceramic properties individually.

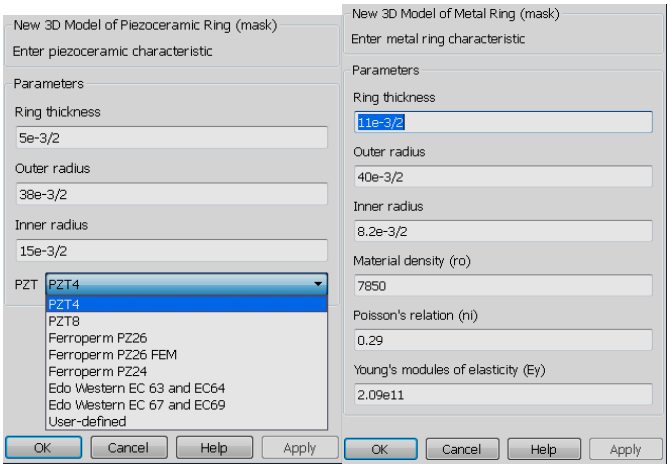

(a) (b)

Fig. 2. Interface for insertion of piezoceramic properties (a) and metal ending properties (b).

If the designation of transducer components adopts the notation shown in Figures 1, and corresponding to the particular block, simulated transducers have the dimensions shown in Table 1.

In order to demonstrate accuracy of the proposed model,

Figure 3 shows the measured frequency characteristic of the ultrasonic transducer under low power level from which it can be seen that the input electrical impedance is in correspondence with the simulated curves.

TABLE 1.
DIMENSIONS OF TRANSDUCER USED IN EXPERIMENTAL ANALYSIS

Dimension (mm)	Thicness	Outer diameter	Inner diameter
Block 3	18	39.8	8
Block 4	0.2	39.8	8
Block 5	11.2	40	13.1
Block 6	0.8	40	13.1
Block 7	11.2	13.1	8
Block 8	8	13.1	8
Block 9	8	8	/
Block 10	21.2	8	/
Block 11	18	8	/

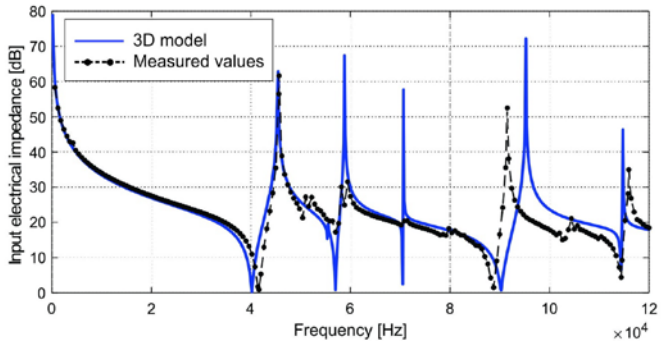

Fig. 3. Simulated and experimental input electrical impedance versus frequency for the ultrasonic transducer.

With small modifications of transducer model, the frequency dependency of mechanical impedance on a free ring-shaped emitter surface can be obtained, which is very important in application where such electromechanical system (transducer) is represented as a sensor or as an energy harvesting device. In the first case, mechanical impedance is calculated when the electrical contacts are short circuit. Therefore, it is essential to first short circuit the electrical contacts (U=0V). The obtained resonant and antiresonant frequencies in the transducer model, when the electrical connections are short circuit, are f_{asc}=19.8kHz and f_{rsc}=40kHz. In the second case, mechanical impedance is calculated when the electrical contacts are left open that is when the input current is zero (I=0A). The obtained resonant and antiresonant frequencies in the transducer model, when the electrical contacts are left open, are f_{aoc}=21.1kHz and f_{roc}=45.3kHz.

The results of this analysis are easily obtained due to the nature of the model implemented in Matlab/Simulink. The frequency error occurs due to the standard material properties of the piezoelectric elements and the metal endings are used in the theoretical calculation and the mechanical and the dielectric losses in the composite transducer are ignored. All above presented results, obtained from model and measurements, are for piezoceramics electrically connected in parallel.

IV. CONCLUSION

The ideal model, which takes into the account all parameters, boundary conditions, all existing resonant modes and conditions based on which the sandwich transducer properties depend, cannot be even realized. Therefore, the presented analysis sought to obtain as comprehensive as possible, but yet simple model, which, although it is approximate, takes into the consideration as much beginning parameters as possible. It is shown that, although the transducer properties depend on many parameters, the greatest impact has the length (thickness) of all transducer components. Based on the presented model, it is possible to synthesize the transducer with predefined properties and given resonant frequency, which was in fact the aim of the presented analysis. Based on the results obtained by applying the proposed transducer models, several transducers that were not presented in this paper were realized. All of them have been tested in many applications. The measurement results of the electrical properties of the obtained electromechanical systems validate this design approach.

ACKNOWLEDGMENT

This work was supported by the Ministry of Education, Science and Technological Development of the Republic of Serbia under the project TR33035.

REFERENCES

[1] P.Langevin, French Patent Nos: 502913 (29.5.1920); 505703 (5.8.1920); 575435 (30.7.1924).
[2] Z. Wang, J. Zeng, H. Song, F. Li, “Research on ultrasonic excitation for the removal of drilling fluid plug, paraffin deposition plug, polymer plug and inorganic scale plug for near-well ultrasonic processing technology,” Ultrasonics Sonochemistry, vol. 36, pp. 162-167, May 2017.
[3] J. Li, T. Monaghanb, T. T. Nguyenb, R. W. Kayc, R. J. Frielb, R. A. Harris, “Multifunctional metal matrix composites with embedded printed electrical materials fabricated by ultrasonic additive manufacturing,” Composites Part B: Engineering, vol. 113, pp. 342-354, Mar. 2017.
[4] S. Kumar, C. S. Wu, G. K. Padhy, W. Ding, “Application of ultrasonic vibrations in welding and metal processing: A status review,” Journal of Manufacturing Processes, vol. 26, pp. 295–322, Apr. 2017.
[5] N. Pokhrel, P. K. Vabbina, N. Pala, “Sonochemistry: Science and Engineering,” Ultrasonics Sonochemistry, vol. 29, pp. 104-128, Mar. 2016.
[6] K. Gotoh, K. Harayama, “Application of ultrasound to textiles washing in aqueous solutions,” Ultrasonics Sonochemistry, vol. 20, no. 2, pp. 747-753, Mar. 2013.
[7] N. N. Mahamuni, Y. G. Adewuyi, “Advanced oxidation processes (AOPs) involving ultrasound for waste water treatment: A review with emphasis on cost estimation,” Ultrasonics Sonochemistry, vol. 17, no.6, pp. 990-1003, Aug. 2010.
[8] S. Lin, H. Tian, “Study on the Sandwich Piezoelectric Ceramic Ultrasonic Transducer in Thickness Vibration,” Smart Materials and Structures, vol. 17, no. 1, pp. 1-9, Jan. 2008.
[9] D. Mančić, G. Stančić, “New Three-dimensional Matrix Models of the Ultrasonic Sandwich Transducers,” Journal of Sandwich Structures and Materials, vol. 12, pp. 63-80, Jan. 2010.
[10] I. Jovanović, D. Mančić, V. Paunović, M. Radmanović, Z. Petrušić, A Matlab/Simulink Model of Piezoceramic Ring for Transducer Design, ICEST 2011, 3, 952-955 (2011).

[11] I. Jovanović, D. Mančić, V. Paunović, M. Radmanović, V.V. Mitić, Metal Rings and Discs Matlab/Simulink 3D Model for Ultrasonic Sandwich Transducer Design, Science of Sintering 44, 287-298 (2012).
[12] Five piezoelectric ceramics, (Bulletin 66011/F, Vernitron Ltd., 1976).